

See discussions, stats, and author profiles for this publication at: <https://www.researchgate.net/publication/231669807>

# Chromia on silica and alumina catalysts: surface structural consequences of interfacial events in the impregnation course of aquated chromium(III) ions

ARTICLE *in* LANGMUIR · FEBRUARY 1992

Impact Factor: 4.46 · DOI: 10.1021/la00038a069

---

CITATIONS

11

READS

39

## 4 AUTHORS, INCLUDING:



Mohamed I Zaki

Minia University

188 PUBLICATIONS 3,593 CITATIONS

[SEE PROFILE](#)



Seham A. A. Mansour

Minia University

43 PUBLICATIONS 562 CITATIONS

[SEE PROFILE](#)



Gamal Mekhemer

Minia University

37 PUBLICATIONS 678 CITATIONS

[SEE PROFILE](#)

# Chromia on Silica and Alumina Catalysts: Surface Structural Consequences of Interfacial Events in the Impregnation Course of Aquated Cr(III) Ions

M. I. Zaki,\* S. A. A. Mansour, F. Taha, and G. A. H. Mekhemer

*Chemistry Department, Faculty of Science, Minia University, El-Minia 61519, Egypt*

*Received April 15, 1991. In Final Form: September 13, 1991*

The impregnation of aquated Cr(III) ions onto silica, alumina, and silica-modified alumina was studied by means of zeta potential and adsorption measurements. The adsorbed Cr species were characterized by UV-vis diffuse reflectance and X-ray diffraction techniques before and after calcination. On silica, the active phase was found to form dominantly crystalline  $\alpha$ -Cr<sub>2</sub>O<sub>3</sub> particles exposing largely oxidized surfaces. On alumina, the formation of highly dispersed chromate species was observed. These considerably different surface structures are related to the different surface hydroxyls properties of the supports.

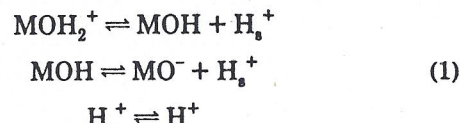
## I. Introduction

Loading a catalyst on an inert but high surface area support improves the accessibility of the active phase.<sup>1</sup> The loading is carried out by impregnation with aquated catalyst precursor species, or by vapor-phase deposition.<sup>1</sup> Recently, another technique has been developed,<sup>2</sup> whereby the catalyst precursor is spread, in the solid state, over the support surface (solid/solid wetting catalysts). However, the impregnation method is the most widely adopted for the preparation of industrial catalysts<sup>3</sup> for economic and technological reasons.

The interfacial chemistry established during the impregnation process involves essentially colloidal and coordination chemical events. The colloidal events are related to the amphoteric interactions between the surface groups of the support and the surrounding aqueous medium.<sup>4</sup> On the other hand, the coordination events are those responsible for the formation of stable surface complexes as a result of interactions between the amphoteric surface groups and aquated catalyst precursor species.<sup>5,6</sup> The thermochemical behavior of these surface complexes, during subsequent high-temperature treatments, controls the dispersion<sup>1</sup> and the radial concentration profile<sup>7</sup> of the active phase in the final catalyst particles.

Research is actively performed on the impregnation course of supported catalysts. The principal objectives are (i) the development of support materials with controlled concentration of amphoteric surface groups<sup>8</sup> and (ii) the scale-up of preparative conditions for maximization of the adsorption selectivity.<sup>9</sup> The accomplishment of these objectives necessitates a deep understanding of the solution chemistry and the surface chemistry of the support.

For SiO<sub>2</sub>, Al<sub>2</sub>O<sub>3</sub>, and SiO<sub>2</sub>-Al<sub>2</sub>O<sub>3</sub>, the most widely used supports, the following has been found. The surface groups in aqueous media are MOH, MO<sup>-</sup>, and MOH<sub>2</sub><sup>+</sup>, where M stands for the metal sites. The relative abundance of these groups is determined by the direction and extent to which the following amphoteric equilibria are shifted



where H<sub>s</sub><sup>+</sup> and H<sup>+</sup> are hydrogen ions on the surface and in the solution bulk, respectively. These equilibria, which also determine the net surface charge of the support, are dependent on the pH<sup>9</sup> and temperature<sup>8</sup> of the impregnating solution. The isoelectric point (IEP) is in the range of pH = 1.8–2.2 for SiO<sub>2</sub>, 4–5 for SiO<sub>2</sub>-Al<sub>2</sub>O<sub>3</sub>, and 7.5–8.6 for Al<sub>2</sub>O<sub>3</sub>, depending on preparation and pretreatment conditions.<sup>10</sup> The adsorption of anionic precursors from solution occurs at pH < IEP, whereas that of cationic species maximizes at pH > IEP.<sup>9</sup> The adsorption of basic (Na<sup>+</sup>, Li<sup>+</sup>) and acidic (F<sup>-</sup>, Cl<sup>-</sup>) ions<sup>11–13</sup> respectively increases and decreases the IEP values of the supports.

Effects of the solution pH and ionic modifiers on the supports have been examined<sup>13–16</sup> during impregnation of the HDS catalyst precursor (i.e. Mo<sub>x</sub>O<sub>y</sub><sup>n-</sup>/Al<sub>2</sub>O<sub>3</sub>). The results are in line with the above-mentioned considerations. It follows that a close relationship exists between the catalyst surface structure and the interfacial events occurring.<sup>14,16</sup> The adsorption behavior of molybdate species on the support has been found to be better explained with an electrostatic model<sup>9</sup> than with ligand exchange assumptions.<sup>6,17</sup>

Similar examinations have been carried out on the methanation catalyst (supported WO<sub>x</sub>), e.g. ref 15, but studies

\* Author to whom all correspondence should be addressed.

(1) Acres, G. J. K.; Bird, A. J.; Jenkins, J. W.; King, F. In *Preparation of Catalysts II*; Delmon, B., Eds.; Elsevier: Amsterdam, 1979; pp 1–30.

(2) Knözinger, H. *Mater. Sci. Forum* 1988, 25–26, 233.

(3) Trimm, D. L. *Design of Industrial Catalysts*; Chemical Engineering Monographs; Elsevier: Amsterdam, 1980; Vol. 11.

(4) Parfitt, G. D. *Pure Appl. Chem.* 1976, 48, 415.

(5) Che, M.; Bonneviot, L. *Pure Appl. Chem.* 1987, 27, 1.

(6) Davis, J. A.; James, R. O.; Leckie, J. O. *J. Colloids Interface Sci.* 1978, 63, 480.

(7) Fujiyama, T.; Otsuka, M.; Tsuiki, H.; Ueno, A. *J. Catal.* 1987, 104, 323.

(8) Akratopulu, K. Ch.; Vordonis, L.; Lycurghiotis, A. *J. Chem. Soc., Faraday Trans. 1* 1986, 82, 3697.

(9) Brunelle, J. P. *Pure Appl. Chem.* 1978, 50, 1211.

(10) Parks, G. A. *Chem. Rev.* 1965, 65, 177.

(11) Akratopulu, K. Ch.; Vordonis, L.; Lycurghiotis, A. *J. Catal.* 1988, 109, 41.

(12) Mieth, J. A.; Schwarz, J. A.; Hung, Y.-J.; Fung, S. C. *J. Catal.* 1990, 122, 202.

(13) Mulcahy, F. M.; Houalla, M.; Hercules, D. M. *J. Catal.* 1987, 106, 210.

(14) Wang, Li.; Hall, W. K. *J. Catal.* 1982, 77, 232.

(15) Mulcahy, F. M.; Houalla, M.; Hercules, D. M. In *Proceedings of the 9th International Congress on Catalysis*; Philips, M. J., Ternan, M., Eds.; The Chemical Institute of Canada: Ottawa, Ontario, 1988; Vol. 4, p 1968.

(16) Caceres, C. V.; Fierro, J. L. G.; Lopez Agudo, A.; Blanco, M. N.; Thomas, H. J. *J. Catal.* 1985, 95, 501.

(17) Hachiya, K.; Sasaki, M.; Saruta, Y.; Mikami, N.; Yasunaga, T. *J. Phys. Chem.* 1984, 88, 23.

on chromia-based polymerization ( $\text{CrO}_x/\text{SiO}_2$ ) and redox ( $\text{CrO}_x/\text{Al}_2\text{O}_3$ ) catalysts are hardly encountered in the literature.<sup>18,19</sup> As a matter of fact, characterization studies (e.g., ref 20) performed on supported chromia have implied that the support surface chemistry plays a critical role in the catalyst surface structure.

The present investigation aims at revealing whether the physical attributes of the surface structure of a supported catalyst evolve from the primary interfacial events occurring during the course of preparation. Therefore, the impregnation course of aquated Cr(III) ions onto  $\text{SiO}_2$ ,  $\text{Al}_2\text{O}_3$ , and  $\text{SiO}_2$ -modified  $\text{Al}_2\text{O}_3$  supports was explored, and the results will be correlated with the surface structures of the final catalysts.

## II. Experimental Section

**A. Cr(III) Impregnating Solution.** Cr(III) solutions with concentrations in the range  $C_i = 0.0032\text{--}0.6 \text{ M}$  were prepared by dissolving  $\text{Cr}(\text{NO}_3)_3 \cdot 9\text{H}_2\text{O}$  (99.9% pure, BDH) in bidistilled water. Intentionally, the ionic strength was not kept constant to avoid foreign additives (e.g.,  $\text{NaNO}_3$ ) in compliance with catalyst preparation requirements.<sup>1</sup> The solutions were acidic ( $\text{pH}_i \leq 3.6$ ), and the acidity increased with increasing concentration (see Figure 2).

Aqueous solutions of Cr(III) provide positively charged hexa-aquo ions ( $(\text{Cr}(\text{H}_2\text{O})_6)^{3+}$ , denoted  $\text{Cr}_{aq}^{3+}$ ).<sup>21</sup> The pH range furnished ( $\text{pH} \leq 3.6$ ), indicates that these ions are hydrolyzed to  $(\text{Cr}(\text{H}_2\text{O})_5(\text{OH}))^{2+}$ ,<sup>21</sup> denoted  $\text{Cr}_{aq}(\text{OH})^{2+}$ .

**B. Support Materials.**  $\text{SiO}_2$ ,  $\gamma\text{-Al}_2\text{O}_3$ , and 3 wt %  $\text{SiO}_2$  modified  $\text{Al}_2\text{O}_3$ , denoted in the text by Si, Al, and SiAl, respectively, were obtained from Degussa (Aerosil-200) and Akzo Chemie (SiAl) and were used as supplied. Al was obtained from an alumina gel by calcination at  $450^\circ\text{C}$  for 5 h in an atmosphere of air. The gel was prepared, according to Lippens,<sup>22</sup> by a drop-wise addition of a (1:1) solution of ammonium hydroxide (AR grade, Prolabo) to a 0.1 M solution of  $\text{Al}(\text{NO}_3)_3 \cdot 9\text{H}_2\text{O}$  (AR grade, BDH) with continuous stirring, until  $\text{pH} \approx 8$  is reached. The gel thus formed was maintained in contact with the mother liquor for 24 h, washed with distilled water until  $\text{NO}_3^-$  free, filtered, and dried at  $120^\circ\text{C}$  until constant weight (96 h). The dried material was ground to 250 mesh and kept dry over  $\text{P}_2\text{O}_5$ .

**C. Impregnation Procedure.** Typically, a 2-g portion of the support was immersed in a 60-mL aliquot of the impregnating solution. The suspension was shaken continuously for 3 h, using a water thermostated ( $25^\circ\text{C}$ ) Kotterman shaker (Germany), and held still for 24 h. Subsequently, the equilibrium pH ( $\text{pH}_{eq}$ ) was determined, and the suspension components were separated by centrifugation. The solid component was thoroughly washed with distilled water to eliminate weakly held Cr(III) species. Then, it was dried at  $60^\circ\text{C}$  until constant weight (48 h). The washing liquid was added to the initial filtrate, and the volume was made up to a total of 100 mL by distilled water.

For simplicity, the impregnated materials are denoted as  $x\text{CrSi}$  which means  $\text{SiO}_2$  impregnated with  $x$  wt % Cr, and similarly for alumina and silica-alumina.

**D. Cr(III) Adsorption Measurement.** The Cr content of the filtrate ( $C_{eq}$ ) was colorimetrically determined<sup>23</sup> at  $\lambda_{max} = 420 \text{ nm}$ , using a Spekol Carl-Zeiss spectrophotometer. The amount of Cr adsorbed (millimoles of Cr/grams of support) was determined by subtracting  $\text{Cr}_{eq}$  from the initial concentration ( $C_i$ ) of the impregnating solution. The Cr loading (wt % Cr) was found to be within  $\pm 0.1\%$  of that determined by means of X-ray

(18) D'Aniello, M. J. *J. Catal.* 1981, 69, 9.

(19) Mishra, R. K.; Mundhara, G. L.; Jain, V. K. *Surf. Technol.* 1985, 26, 315.

(20) (a) Zaki, M. I.; Fouad, N. E.; Leyrer, J.; Knözinger, H. *Appl. Catal.* 1986, 21, 359. (b) Hardcastle, F. D.; Wachs, I. E. *J. Mol. Catal.* 1988, 46, 173. (c) Fouad, N. E.; Knözinger, H.; Zaki, M. I.; Mansour, S. A. A. Z. *Phys. Chem. in press.* (d) McDaniel, M. P. *J. Catal.* 1982, 76, 37.

(21) Rollinson, C. L. In *Comprehensive Inorganic Chemistry*; Bailar, J. C., et al., Eds.; Pergamon Press: Oxford, 1975; Vol. 3, pp 676–699.

(22) Lippens, B. C. Ph.D. Thesis, Delft University, The Netherlands, 1967.

(23) Deren, J.; Haber, J.; Podgorreck, A.; Burzyk, J. *J. Catal.* 1963, 2, 161.

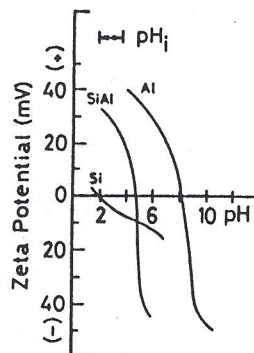


Figure 1. pH dependences of  $\zeta$  potential (mV) in aqueous suspensions of the support materials. The figure indicates the pH range ( $\text{pH}_i$ ) furnished by Cr(III) impregnating solutions.

fluorescence on a few selected samples. The reference materials were physical mixtures of chromium nitrate and the support.

**E. Zeta Potential Measurement.** The zeta ( $\zeta$ ) potentials of the unimpregnated and impregnated supports immersed in water were measured as a function of the pH of the medium, using a Rank Mark-II microelectrophoresis instrument. The pH was adjusted using HCl and KOH solutions. From the measured electrophoretic mobility, the  $\zeta$  potential was calculated by the equation<sup>24</sup>

$$\zeta = 4\pi\eta u/eE \quad (2)$$

where  $\eta$  is the viscosity coefficient of the solution surrounding the colloid particles,  $u$  is the electrophoretic velocity,  $E$  is the strength of the applied field, and  $\epsilon$  is the dielectric constant of the medium.

**F. Spectroscopic Analyses.** UV-vis diffuse reflectance spectroscopy (DR) and X-ray diffractometry (XRD) were used to monitor surface and bulk structures of the unimpregnated and impregnated supports, as well as the final catalysts. The catalysts were obtained by calcination at  $600^\circ\text{C}$  for 5 h of the impregnated supports;<sup>20c</sup> they are indicated in the text by adding C to the symbols of the parent impregnated supports.

DR spectra were recorded over a wavelength range from 900 to 190 nm on a Lambda 15 double-beam Perkin-Elmer spectrophotometer equipped with a diffuse reflectance attachment. The support materials were used as references for each series of impregnated supports and supported catalysts, whereas speccpure  $\text{BaSO}_4$  was the reference material for the unimpregnated supports. The DR spectra were not used for quantitative measurements; therefore, they were not converted to the Kubelka-Munk function.<sup>25</sup>

XRD powder diffractograms were recorded by means of a Model JSX-60PA Jeol diffractometer. Ni-filtered  $\text{Cu K}\alpha$  radiation (35 kV and 30 mA) was used. The diffractometer was operated with  $20^\circ$  diverging and receiving slits at a scan rate of 20 mm/min and a continuous intensity trace was recorded as a function of  $2\theta$ . The test samples, ground to a particle size of  $\leq 44 \mu\text{m}$  and packed into the well of a sample holder, were mounted in a horizontal position. The diffraction patterns ( $I/I_0$  vs  $d$  spacing ( $\text{\AA}$ )) were compared with the ASTM standards,<sup>26</sup> for identification purposes.

## III. Results and Discussion

**A. pH Dependence of Support Zeta Potential.**  $\zeta$ -pH plots for the unimpregnated supports are shown in Figure 1. The IEP values thereby determined are compared with literature data in Table I. The comparison reveals an excellent agreement.

(24) Wiersema, P. H.; Loeb, A. L.; Overbeck, J. Th. G. *J. Colloid Interface Sci.* 1966, 22, 78.

(25) Schoonheydt, R. A. In *Characterization of Heterogeneous Catalysts*; Delannay, F., Ed.; Marcel Dekker: New York, 1981; pp 125–167.

(26) *X-ray Powder Data File*; Smith, J. V., Ed.; American Society for Testing and Materials: Philadelphia, PA, 1960.

(27) Kita, H.; Henmi, N.; Shimazu, K.; Hattori, H.; Tanabe, K. *J. Chem. Soc., Faraday Trans. 1* 1981, 77, 2451.

Table I. Isoelectric Point (IEP) and Surface Area ( $S_{BET}$ ) of Unimpregnated Support Materials

material	$S_{BET}$ , <sup>a</sup> m <sup>2</sup> /g	IEP ( $\pm 0.1$ )	
		present work	previous work (ref)
Si	200	1.9	1.8–2.2 (10)
Al	214	8.2	7.5–8.6 (10)
SiAl	460	4.6	4.6 (27) <sup>b</sup>

<sup>a</sup> Determined from nitrogen adsorption data obtained at liquid nitrogen temperature. <sup>b</sup> According to ref 27, a commercially available SiAl (N-631(L), Nikki Chemical Co., Japan) was used.

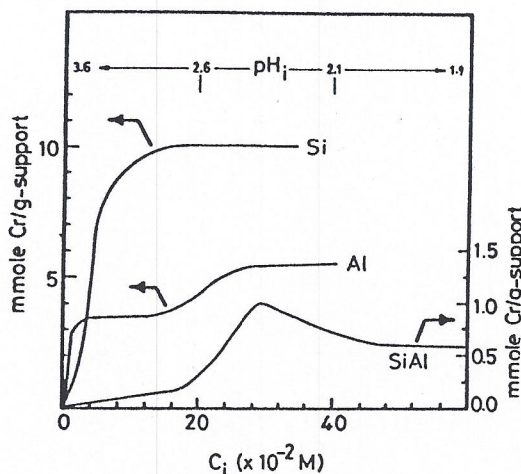


Figure 2. Cr(III) adsorption isotherms (at 25 °C) determined on the support materials. The figure indicates  $pH_i$  values corresponding to the  $C_i$  values of the impregnating solutions.

The low value ( $=1.9$ ) of Si IEP is indicative of acidic surface groups ( $\text{SiOH}$ ).<sup>10</sup> Figure 1 reveals that in the pH range of the impregnating solutions ( $pH_i = 3.6$ –1.9) the Si surface is zero to slightly negatively charged, due to deprotonation of  $\text{SiOH}$  to  $\text{SiO}^-$  groups.<sup>10</sup> It has been reported previously<sup>2</sup> that appreciable deprotonation only occurs above  $\text{pH} = 6$ . Accordingly,  $\text{SiOH}$  is considered to act as a weak acid ( $pK_a = 9$ ).<sup>28</sup>

The Al IEP assumes a much higher value ( $=8.2$ ) than the Si IEP does. As a result, the surface acquires a net positive charge, due most likely to  $\text{AlOH}$  protonation to  $\text{AlOH}_2^+$  groups, at the  $pH_i$  range furnished (Figure 1). It also suggests that at  $\text{pH} > \text{IEP}$   $\text{AlOH}$  deprotonates to  $\text{AlO}^-$ , thus giving rise to the negative  $\zeta$ -potential values observed. It is obvious, however, that the rate of  $\text{AlOH}$  deprotonation ( $(\Delta\zeta(-\text{mV})/\Delta\text{pH})$ ) is higher than that ( $(\Delta\zeta(+\text{mV})/\Delta\text{pH})$ ) of the protonation.

SiAl shows IEP value ( $=4.6$ ) intermediate between the values of Al and Si. Thus, the amphoteric surface groups are stronger and weaker acids than  $\text{AlOH}$  and  $\text{SiOH}$ , respectively. These results indicate that the minor  $\text{SiO}_2$  component (3 wt %) modifies notably the surface chemistry of the major  $\text{Al}_2\text{O}_3$  component. Moreover, Figure 1 indicates that at the  $pH_i$  range furnished, positively charged surfaces are exposed, i.e. similar to Al.

**B. Support Adsorptive Behavior toward Cr(III).** Cr(III) adsorption isotherms determined on the various supports are shown in Figure 2. Data therefrom derived are summarized in Table II.

**1. Silica.** Figure 2 shows that the amount of Cr adsorbed increases with  $C_i$  to a value of 10 mmol of Cr/g of support at  $C_i \geq 20 \times 10^{-2}$  M ( $pH_i \leq 2.8$ ). Table II shows the corresponding maximum loading of 51 wt % Cr and an intrinsic uptake of 29 Cr/nm<sup>2</sup>. Calculations based on the maximum intrinsic uptake and on the reported<sup>29</sup>

(28) Corent, D.; Burwell, R. L., Jr. *J. Am. Chem. Soc.* 1968, 90, 2489.

Table II. Data Derived from Cr(III) Adsorption Isotherms on Support Materials

material	ultimate loading, wt % Cr	intrinsic uptake <sup>a</sup> (no. of Cr ions per nm <sup>2</sup> )
Si	41	23
	51	29
Al	16	9
	28	15
SiAl	1	<1
	3	<1
	5	1

<sup>a</sup> Calculated on basis of the specific uptake values (millimoles of Cr/g of support) determined in Figure 2 and the surface area of the support (m<sup>2</sup>/g).

surface-OH population ( $\sim 6 \text{ OH}/\text{nm}^2$ ) give a Cr/OH number ratio close to 5. The  $pH_{eq}$  value, measured following a 24-h contact with the support, was similar to the  $pH_i$  of the impregnating solution. This indicates that the  $\text{H}^+$  concentration in the solution bulk remains almost constant.

Figure 2 also shows that almost 75% of the ultimate uptake of Cr is effected from solutions of  $C_i < 6 \times 10^{-2}$  M ( $pH_i > 3$ ), and as  $C_i$  exceeds this value ( $pH_i < 3$ ) the increase in the amount adsorbed declines markedly. These observations are consistent with the fact that at pH appreciably higher than Si IEP ( $=1.9$ )  $\text{SiOH}$  deprotonates facilitating the formation of electrostatically bound  $\text{SiO}^-:\text{Cr}_{aq}(\text{OH})^{2+}$  species. The nondirectional character of such type of bonding may explain the significantly high Cr/OH ratio determined (ca. 5).

As the  $pH_i$  decreases with a  $C_i$  increase and comes closer to the IEP value, the  $\text{SiOH}$  deprotonation is considerably retrogressed. The consequent decline of the increase of Cr uptake reveals that the adsorption sites are dominantly those generated via the  $\text{SiOH}$  deprotonation. This may present an obvious conflict with a report by Dugger et al.,<sup>30</sup> in which Cr(III) uptake on  $\text{SiO}_2$  at pH  $\sim 2$  has been assigned to an ion exchange process. For a metal complex to be exchanged onto Si surfaces it must have a  $pK_a \geq 9$ .<sup>31</sup> The  $pK_a$  of  $(\text{Cr}(\text{H}_2\text{O})_6)^{3+}$  is 3.8,<sup>21</sup> making it an unlikely candidate for ion exchange.

**2. Alumina.** The isotherm of Al (Figure 2) shows a two-step adsorption process: an initial step at  $C_i < 2 \times 10^{-2}$  M ( $pH_i > 3.4$ ) and a subsequent step at  $C_i > 12 \times 10^{-2}$  M ( $pH_i < 2.8$ ). The amount adsorbed in the first step amounts to 3.5 mmol of Cr/g, whereas that following the second step is 5.5 mmol of Cr/g. This shows that most of the ultimate uptake is effected throughout the initial step. Data derived from these amounts of adsorption are given in Table II. It is worth mentioning that the  $pH_{eq}$  values (4.5–2.2) were slightly higher than the initial values (3.6–1.9). This is most likely due to the dissolution of a minute proportion of the support material.<sup>14</sup>

Table II indicates that the ultimate loading of Cr on Al (28 wt % Cr) is much less than that (51 wt % Cr) on Si. Thus Al has a lower tendency toward Cr(III) than Si. The Cr/OH ratio derived from the ultimate intrinsic uptake (15 Cr/nm<sup>2</sup>) and reported<sup>32</sup> surface-OH population ( $\sim 11 \text{ OH}/\text{nm}^2$ ) for  $\gamma\text{-Al}_2\text{O}_3$  is very close to unity (namely, =1.4).

At the  $pH_i$  range furnished, the Al surface is expected to expose  $\text{AlOH}$  and  $\text{AlOH}_2^+$  groups. Thus, the surface acquires a net positive charge (Figure 1), which does not

(29) Young, G. J. *J. Colloid Sci.* 1985, 13, 67.

(30) Dugger, D. L.; Stanton, J. H.; Irby, B. N.; McConnell, B. I.; Cummings, W. W.; Maatman, R. W. *J. Phys. Chem.* 1964, 68, 32.

(31) Lunsford, J. H.; Fu, S. L.; Myers, D. L. *J. Catal.* 1988, III, 231.

(32) Soled, S. *J. Catal.* 1983, 18, 252.

allow for electrostatic attraction of Cr cations. Accordingly, the Cr uptake occurs most likely through ion exchange. Hachiya,<sup>33</sup> looking at kinetic results of metal ion adsorption on  $\gamma\text{-Al}_2\text{O}_3$ , has come to a similar conclusion. The results indicated, however, that the ion exchange occurs essentially between AlOH groups ( $pK_a = 3.7$ ) and metal ion complexes ( $pK_a \geq 3.7$ ) giving rise to  $\text{AlOM}(\text{H}_2\text{O})^{n+}$  and  $\text{AlOMOH}^{(n-1)+}$  surface species. In accordance with MacBride,<sup>34</sup> Hachiya<sup>33</sup> defined the adsorption as being specific and the AlO-metal bond in the adsorbed state as being partially covalent and strong.

Since the  $pK_a$  value (=3.8) of  $(\text{Cr}(\text{H}_2\text{O})_6)^{3+}$  is favorable, one may accordingly<sup>33</sup> suggest the formation of ion exchanged Cr species,  $\text{AlOCr}_{\text{aq}}(\text{OH})^+$  and  $\text{AlOCr}_{\text{aq}}(\text{OH})_2$ , during the adsorption of Cr. It is tempting to presume that the formation of the neutral species,  $\text{AlOCr}_{\text{aq}}(\text{OH})_2$ , occurs preferably during the initial adsorption step (low  $C_i$  and high pH). The decline of Cr uptake from highly concentrated solutions (Figure 2) is most probably associated with the dominance of  $\text{AlOH}_2^+$  surface groups under these conditions. The specificity of Cr adsorption on Al can also be inferred from the Cr/OH ratio (~ unity), for it is compatible with the directional character of the prevailing type of bonding to the surface.

**3. Silica-Modified Alumina.** The adsorption isotherm of SiAl is radically different from those determined on Si and Al (Figure 2). It shows a very weak Cr adsorption at  $C_i < 20 \times 10^{-2}$  M ( $\text{pH}_i > 2.8$ ), and a peak near  $C_i$  of  $30 \times 10^{-2}$  M ( $\text{pH}_i = 2.2$ ). At higher  $C_i$  values ( $\text{pH}_i < 2.2$ ), the amount adsorbed decreases to a constant value of 0.6 mmol of Cr/g, whereas the peak corresponds to 1.0 mmol of Cr/g. Table II indicates that the corresponding loadings are 3 and 5 wt % Cr, respectively.

The above results reveal that the  $\text{SiO}_2$  component (3 wt %) suppresses considerably the Cr adsorption tendency of Al making SiAl the weakest Cr adsorbent of the three supports, although the surface area of SiAl is twice that of Si and Al (Table I). A surface analysis of  $\text{SiO}_2$ -modified aluminas,<sup>35</sup> by means of secondary ion mass spectrometry (SIMS), has determined a high  $\text{SiO}_2$  surface content for materials containing  $\leq 5$  wt %  $\text{SiO}_2$ . At higher content,  $\text{SiO}_2$  reside dominantly into the bulk of alumina.<sup>35</sup> It follows, that the  $\text{SiO}_2$  forms a coating on Al, in line with Iler.<sup>36</sup> Compatibly, IR hydroxyl spectra taken from low  $\text{SiO}_2$  ( $\leq 5$  wt %) SiAl samples show evidence of  $\text{SiOH}$  and  $\text{AlOH}$  surface groups.<sup>37</sup> A preliminary IR analysis of our SiAl also detected absorptions due to free  $\text{SiOH}$  and  $\text{AlOH}$  groups. Accordingly, one may convincingly consider the SIMS results applicable to the present sample.

In view of these considerations, the Cr adsorption on SiAl can be explained on the basis of a heterogeneous surface chemistry. The net surface positive charge generated at the  $\text{pH}_i$  range furnished ( $\leq 3.6$ ) accounts, as indicated in Figure 1, for the formation of  $\text{SiOH}_2^+$  and  $\text{AlOH}_2^+$ , with the former groups being more dominant. The inability of the aquated Cr complexes to exchange for the silanol proton, as discussed above, may explain the notably weak tendency of SiAl toward Cr adsorption. In the mean time, the minor adsorption observed (Figure 2) would result in the formation of electrostatically bound species onto silica surfaces and, to a much lesser extent, onto alumina surfaces.

(33) Hachiya, K. *J. Sci. Hiroshima Univ.* 1981, 45, 141.  
(34) MacBride, M. B. *Soil. Sci. Soc. Am. J.* 1978, 42, 27.  
(35) Espie, A. W.; Vickerman, J. C. *J. Chem. Soc., Faraday Trans. 1* 1984, 80, 1903.

(36) Iler, R. K. *J. Am. Ceram. Soc.* 1964, 47, 339.

(37) Baumgarten, E.; Zachos, A. *Spectrochim. Acta, Part A* 1981, 37A, 757.

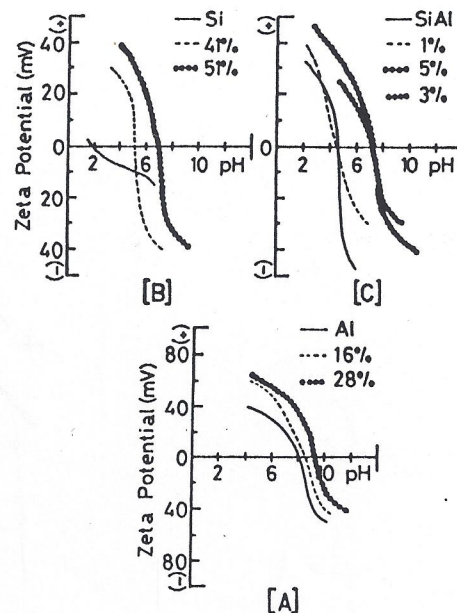


Figure 3. pH dependences of  $\zeta$  potential in aqueous suspensions of 60 °C dried Cr(III) impregnated supports at the loading levels indicated. The results obtained for the unimpregnated supports are inset for comparison purposes.

**B. Characteristics of Loaded Cr Species.** Some 60 °C dried impregnated support samples, selected carefully to represent the various Cr adsorption steps monitored by the isotherms (Figure 2), were subjected to  $\zeta$  potential, XRD, and DRS measurements. Catalysts, obtained by calcination at 600 °C for 3 h, were also analyzed by XRD and DRS.

**1. Impregnated Supports.**  $\zeta$ -pH plots, shown in Figure 3B, indicate that loading of Cr on Si shifts the support IEP (=1.9) to significantly higher values (to 5.2–6.8). This behavior is maintained by Cr on SiAl (Figure 3C), except at the lowest loading observed (1 wt % Cr). On the other hand, Cr on Al insignificantly increases the support IEP value (from 8.2 to 9.3) (Figure 3A). These results reveal<sup>33</sup> that Cr on Al is potential determining, whereas on Si and SiAl it is not. According to Hachiya,<sup>33</sup> this may infer that Cr ions on Al occur on nearly the same adsorption plane as  $\text{H}^+$  ions. This, in fact, can well be fulfilled for by the  $\text{AlOCr}_{\text{aq}}(\text{OH})^+$  species suggested to form via ion exchange onto Al, but not by the weak electrostatically bound  $\text{SiO}^-:\text{Cr}_{\text{eq}}(\text{OH})^{2+}$  species on Si or SiAl. Therefore, Cr has been considered<sup>33</sup> to adsorb specifically on alumina, but nonspecifically on silica surfaces.

XRD patterns obtained for all impregnated samples displayed nothing but the characteristic pattern of the supports. Thus, the impregnated Cr species are highly dispersed and do not form bulk phases, at least at a detectable level. Moreover, the fact that the support bulk structures remain unmodified may help suggesting that the impregnated species reside essentially on the surface.

Irrespective of the support material and the loading level, the DR spectra (Figure 4) display the same band structure. It consists of two strong d-d absorptions at 430 ( $\text{A}_{2g} \rightarrow \text{T}_{1g}$ ) and 600 nm ( $\text{A}_{2g} \rightarrow \text{T}_{2g}$ ), and a shoulder at 680 nm. The absorption bands are due to  $\text{Cr}^{3+}$  in octahedral coordination,<sup>38</sup> whereas the shoulder is presumably associated with slightly oxidized Cr (to Cr(IV) or Cr(V)).<sup>38</sup> Cr(III) is easily oxidizable when heated in air even at

(38) Cimino, A.; De Angelis, B. A.; Luchetti, A.; Minelli, G. *J. Catal.* 1976, 45, 316.

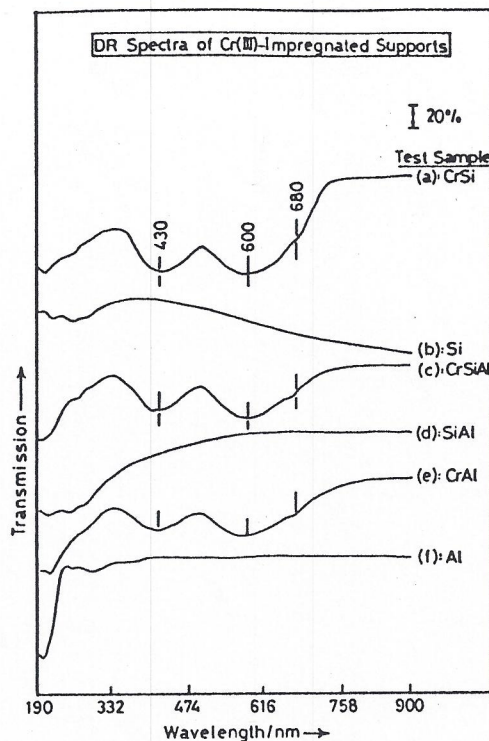


**Figure 4.** Typical DR spectra taken from the various impregnated support materials. The figure insets the spectra exhibited by the unimpregnated supports for comparison purposes.

temperatures as low as 60 °C.<sup>39</sup> The DR examination reveals, therefore, that irrespective of the support used and the loading level achieved, Cr species remain dominantly in the trivalent oxidation state, assuming octahedral coordination environment.

**2. Supported Catalysts.** XRD diffractograms shown by the Al<sub>2</sub>O<sub>3</sub>-supported catalysts (Figure 5g), loaded up to the highest level reached (28 wt % Cr), display nothing but the characteristic pattern of the support (Figure 5h). This indicates that the high state of dispersion observed for the parent-impregnated samples is maintained by the catalysts regardless of the high temperature calcination experienced. However, the DR spectral features of the impregnated samples (Figure 4e) are not maintained by the catalysts (Figure 6c). More precisely, the DR spectra of the catalysts display new absorption bands in the charge transfer (CT) region (<500 nm) and monitor no d-d absorptions (>500 nm). These bands are centered around 270, 370, and 450 nm, and due respectively to <sup>1</sup>A → <sup>1</sup>T<sub>2</sub> ( $1t_1 \rightarrow 7t_2$ ), <sup>1</sup>A<sub>1</sub> → <sup>1</sup>T<sub>2</sub> ( $1t_1 \rightarrow 2e$ ), and <sup>1</sup>A<sub>1</sub> → <sup>1</sup>T<sub>1</sub> ( $1t_1 \rightarrow 2e$ ) CT transitions of chromate species.<sup>40</sup> The appearance of the 450-nm band, which is symmetry forbidden,<sup>40</sup> may imply that the chromates are strongly bound to the support surface. These results indicate that the calcination at 600 °C converts oxidatively the initial Cr(III) to highly dispersed Cr(VI) species anchored to the support surface. The chromates are thermally stabilized on the support, since Cr(VI) compounds are known to decompose to the trivalent state at ≥400 °C.<sup>41</sup>

For the SiO<sub>2</sub>-supported catalysts, XRD diffractograms (Figure 5a,b) show, in addition to the support pattern (Figure 5c), diffraction peaks very similar to those compiled in the ASTM No. 6-0504<sup>26</sup> for the α-Cr<sub>2</sub>O<sub>3</sub> phase. The

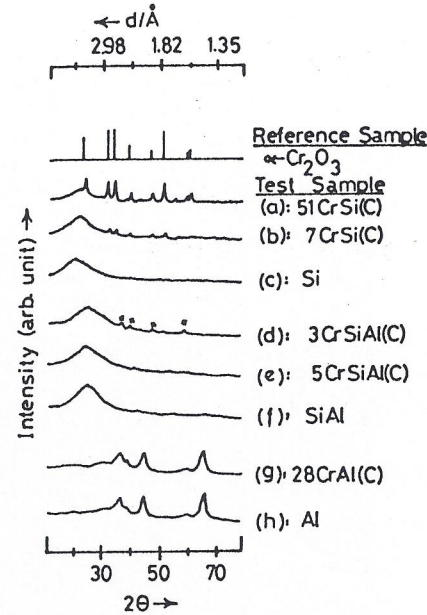


**Figure 5.** X-ray powder diffractograms (Cu K $\alpha$  radiation) obtained for the catalysts produced by 600 °C calcination of the corresponding impregnated supports. The figure insets the diffractograms shown by the unimpregnated supports and a depiction of the ASTM pattern (6-0504) of  $\alpha$ -Cr<sub>2</sub>O<sub>3</sub> for comparison purposes.

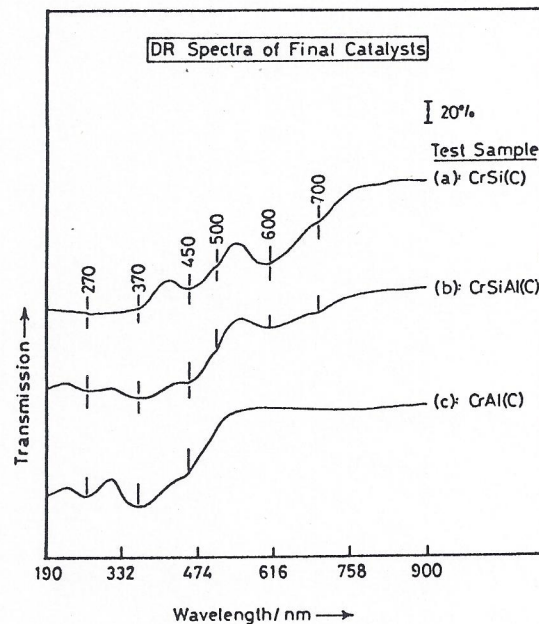


**Figure 6.** Typical DR spectra taken from the various catalyst systems.

corresponding DR spectra (Figure 6a) display CT absorptions due to chromates (at <500 nm), as well as d-d absorptions at 500, 600, and 700 nm. No d-d absorptions are observed for Cr(III) in crystalline Cr<sub>2</sub>O<sub>3</sub>, since they occur (at >1200 nm<sup>20a</sup>) beyond the range of frequencies measured. The absorptions at 600 and 700 nm have been previously attributed to Cr(III) in amorphous clusters.<sup>20a</sup> On the other hand, an absorption in the range 487–578 nm has been considered<sup>40</sup> indicative of a strong excitation from the counteraction to the chromate group and, hence, a high degree of covalency of the Cr–O bonds. The appearance of such an absorption has accordingly been considered<sup>42</sup> to mark the formation of Cr<sup>3+</sup>–O–Cr<sup>6+</sup> bonds, i.e. chromium chromates. In conclusion, the DR results

(39) Burwell, R. L., Jr.; Haller, G. L.; Taylor, K. C.; Read, J. F. *Adv. Catal.* 1969, 20, 1.

(40) Szabo, Z. G.; Kamaras, K.; Szebeni, Sz.; Ruff, I. *Spectrochim. Acta, Part A* 1978, 34A, 607.

(41) Zaki, M. I.; Fahim, R. B. *J. Thermal Anal.* 1986, 31, 825.

may indicate that the initial Cr(III) species on Si are oxidized to chromates which, unlike the case on Al, are decomposed reductively to Cr(III) species. The latter species coexist in crystalline ( $\alpha$ -Cr<sub>2</sub>O<sub>3</sub>) and amorphous structures, and the DR-monitored chromates are stabilized on their surfaces rather than on the support surface.

The case with the catalyst samples supported on SiAl is interesting. The catalyst loaded from a solution corresponding to the uptake maximum (Figure 2), i.e. 5CrSiAl(C), shows an XRD pattern (Figure 5e) similar to that of the support (Figure 5f). In contrast, the catalyst loaded from a solution of a higher concentration, i.e. 3CrSiAl(C), which is effectively of a lower load than the previous one, displays additionally very weak peaks (\*) labeled due to  $\alpha$ -Cr<sub>2</sub>O<sub>3</sub> phase. This behavior resembles that of the SiO<sub>2</sub>-supported catalysts. Consistently, the DR spectra taken from the SiAl-supported catalysts (Figure 6b) are very similar to those taken from the SiO<sub>2</sub>-supported catalysts (Figure 6a). Thus, these results are in line with the adsorption results, in suggesting that the Cr(III) uptake occurs essentially on the silica component of the SiAl support.

**C. Interfacial Events and Surface Structures.** The uptake measurements carried out in the present investigation determine (Table II) much higher Cr loading on silica than on alumina surfaces. On the basis of the  $\zeta$ -potential measurements of the unimpregnated and im-

pregnated supports (Figure 3), the considerably high loadings on Si may be related to nonspecific adsorption, resulting in the formation of electrostatically bound SiO<sup>-</sup>:Cr<sub>aq</sub>(OH)<sup>2+</sup> species. The low loadings on Al may accordingly be related to specific adsorption, leading to the formation of covalently bound AlOCr<sub>aq</sub>(OH)<sup>+</sup> species. The inherently weak, electrostatically bound Cr species on Si would understandably be less stable to the subsequent thermal treatment (at 600 °C) than the partially covalently bound species on Al. This may explain the disparate surface structures revealed (Figures 5 and 6) for the active phase in the final catalysts: large  $\alpha$ -Cr<sub>2</sub>O<sub>3</sub> particles of oxidized surfaces on Si, and highly dispersed chromates on Al.

Recent characterization studies of the catalysts<sup>20b,c,43,44</sup> have reported similar surface structures. These studies have related the surface structural differences observed to the diverse surface-OH chemistries and populations of alumina and silica. In fact, our results are generally in favor of such a correlation. This is in the sense that these surface hydroxyl properties of the support govern critically their amphoteric conduct in solution and the type of bonding of the precursor species to the surface, and, hence, their stability to the subsequent thermal treatment.

Registry No. Cr, 7440-47-3; SiO<sub>2</sub>, 7631-86-9; Al<sub>2</sub>O<sub>3</sub>, 1344-28-1.

(42) Ellison, A.; Oubridge, J. O. V.; Sing, K. S. W. *Trans. Faraday Soc.* 1970, 66, 1004. Ellison, A.; Sing, K. S. W. *J. Chem. Soc., Faraday Trans. 1* 1978, 74, 2807.

(43) Richter, M.; Reich, P.; Ohlmann, G. *J. Mol. Catal.* 1988, 46, 79.

(44) Ellison, A.; Diakun, G.; Worthington, P. *J. Mol. Catal.* 1988, 46, 131.